# Tibiofibular Syndesmotic Ligaments: MR Arthrography in Cadavers with Anatomic Correlation[1]

Mayura Boonthathip, MD
Lina Chen, MD
Debra J. Trudell, RA
Donald L. Resnick, MD

**Purpose:** To use magnetic resonance (MR) imaging and MR arthrography to characterize the normal anatomy of the tibiofibular syndesmotic ligaments with standard and oblique imaging planes in cadavers.

**Materials and Methods:** Ten cadaveric ankle specimens were obtained and used in accordance with institutional and HIPAA guidelines, and informed consent for research was obtained from relatives of the deceased. MR imaging was performed before and after intraarticular administration of contrast material. Proton-density-weighted MR images were correlated with anatomic slices.

**Results:** The anterior inferior tibiofibular ligament (AITFL) had a variable number of bands in all specimens. A separate distal band was identified in all specimens, revealing a more horizontal course than other components of the AITFL and attaching more medially to the anterior margin of the tibial plafond. The posterior inferior tibiofibular ligament (PITFL) and inferior transverse ligament were best seen in coronal oblique planes. The posterior intermalleolar ligament was observed in all specimens and had a variable appearance that ranged from a thin strand to a thick cord. The interosseous ligament (IOL) coursed obliquely to attach proximally to the tibia and insert distally in the fibula. This ligament was fenestrated with separate anterior and posterior fibers. The anterior fibers were more proximal, and the posterior fibers were more distal, attaching to the fibula in close proximity to the PITFL. Coronal images best depicted the course of the IOL.

**Conclusion:** Oblique imaging planes parallel to the long axis of the ligament better display the normal anatomy of the tibiofibular syndesmotic ligaments when compared with standard imaging planes.



[1] From the Department of Radiology, University of California-San Diego, San Diego, Calif; and VA Healthcare System San Diego, 3350 La Jolla Village Dr, La Jolla, CA 92161. Received April 9, 2009; revision requested May 8; revision received July 20; accepted August 4; final version accepted September 29. **Address correspondence to** M.B. (e-mail: *mayura_boon@yahoo.com*).

The articulations between the tibia and fibula can be divided into three regions: the proximal (superior) tibiofibular joint, the interosseous membrane, and the distal (inferior) tibiofibular joint, also known as the tibiofibular syndesmosis. The distal tibiofibular syndesmosis is formed by the rough convex surface of the medial aspect of the lower end of the fibula and the rough concave surface of the lateral aspect of the tibia. Its integrity is fundamental in allowing adequate function of the ankle (1).

The tibiofibular syndesmosis has four ligaments: the anterior inferior tibiofibular ligament (AITFL), posterior inferior tibiofibular ligament (PITFL), inferior transverse ligament (ITL), and interosseous ligament (IOL). Some injuries to the syndesmotic ligaments may lead to instability, which can require surgical stabilization (2,3). Thus, visualization of the syndesmotic ligaments is potentially important for therapeutic decisions.

All four ligaments of the tibiofibular syndesmosis have different orientations, and the angle of their osseous attachments is variable. In one study, researchers described the ability of magnetic resonance (MR) imaging to enable visualization of these ligaments, with a reported sensitivity of 93%–100% and a specificity of 96%–100% in the diagnosis of AITFL injuries (4). In another study, researchers found 100% sensitivity and 93% specificity of MR imaging for this diagnosis (5). In these two studies, researchers used standard MR imaging planes.

The purpose of this study was to use MR arthrography to characterize the normal anatomy of the tibiofibular syndesmotic ligaments with coronal and axial oblique imaging planes in cadavers.

### Advance in Knowledge

- The anatomy of the tibiofibular syndesmotic ligaments is demonstrated and described with an emphasis on the use of these oblique planes.

## Materials and Methods

### Cadaver Specimen Preparation

Ten fresh frozen anatomic specimens of the ankles (seven left ankles, three right ankles) were obtained from four female cadavers (mean age at death, 88.3 years; range, 73–95 years) and four male cadavers (mean age at death, 88.8 years; range, 80–98 years). Both the left ankle and the right ankle were taken from two cadavers. All specimens were obtained and used in accordance with institutional and Health Insurance Portability and Accountability Act guidelines, and informed consent for research was obtained from relatives of the deceased. The cadaveric specimens were frozen at −40°C (Bio-Freezer; Forma Scientific, Marietta, Ohio). The specimens contained the entire foot above the ankle joint, including the distal third of the tibia and fibula. Routine radiographs were obtained to ensure that the ankle joint was not affected by surgical alterations or gross pathologic abnormalities, such as fractures. They were allowed to thaw for 24 hours at room temperature before MR imaging.

### MR Imaging and MR Arthrography

MR images were acquired with a 1.5-T imager (Signa LX Horizon, version 8.3; GE Healthcare, Waukesha, Wis) and use of a standard ankle coil. All ankle specimens were imaged with the ankle in a neutral position. Imaging was first performed in the standard axial, coronal, and sagittal planes. Subsequently, coronal oblique planes for the AITFL, PITFL, and ITL were prescribed by using standard axial planes parallel to the orientation of each of the individual ligaments. The axial oblique planes were prescribed by using coronal oblique planes parallel to the orientation of the individual ligaments. A total of nine sequences were performed for each specimen (Fig 1).

To fully distend the ankle joint, approximately 8–19 mL of a mixture of gadopentetate dimeglumine (Magnevist; Bayer Schering Pharma, Berlin, Germany) and saline solution (1:200 dilution) was injected into the joint with fluoroscopic guidance by using a 20-gauge needle and an anteromedial approach. MR imaging was performed within 15 minutes after the injection.

The MR imaging protocol consisted of fast spin-echo proton-density-weighted sequences (repetition time msec/echo time msec, 3000/10; echo train length, eight; field of view, 11; section thickness, 2.5 mm; no intersection gap; imaging matrix, 256 × 256; number of signals acquired, two; bandwidth, 20 MHz). Images were acquired without fat suppression before and after intraarticular administration of a dilute gadolinium-containing contrast agent.

### MR Imaging Measurements

All measurements were obtained by using electronic calipers (Impax software, version 5.2; Agfa Healthcare, Ridgefield Park, NJ). Measurements were obtained three times by the same person (M.B., 1 year of general radiology and 2 years of musculoskeletal imaging fellowship), and the average values were determined. Coronal oblique planes for

### Implication for Patient Care

- Oblique MR imaging planes programmed to be parallel to the long axis of each ligament can be used to optimize visualization of the tibiofibular syndesmotic ligaments.

**Published online**
10.1148/radiol.09090624

**Radiology 2010;** 254:827–836

**Abbreviations:**
AITFL = anterior inferior tibiofibular ligament
IML = intermalleolar ligament
IOL = interosseous ligament
ITL = inferior transverse ligament
PITFL = posterior inferior tibiofibular ligament
PTFL = posterior talofibular ligament

**Author contributions:**
Guarantors of integrity of entire study, M.B., D.L.R.; study concepts/study design or data acquisition or data analysis/interpretation, all authors; manuscript drafting or manuscript revision for important intellectual content, all authors; manuscript final version approval, all authors; literature research, M.B.; experimental studies, L.C., D.J.T.; and manuscript editing, M.B., L.C., D.L.R.

Authors stated no financial relationship to disclose.

**Figure 1**

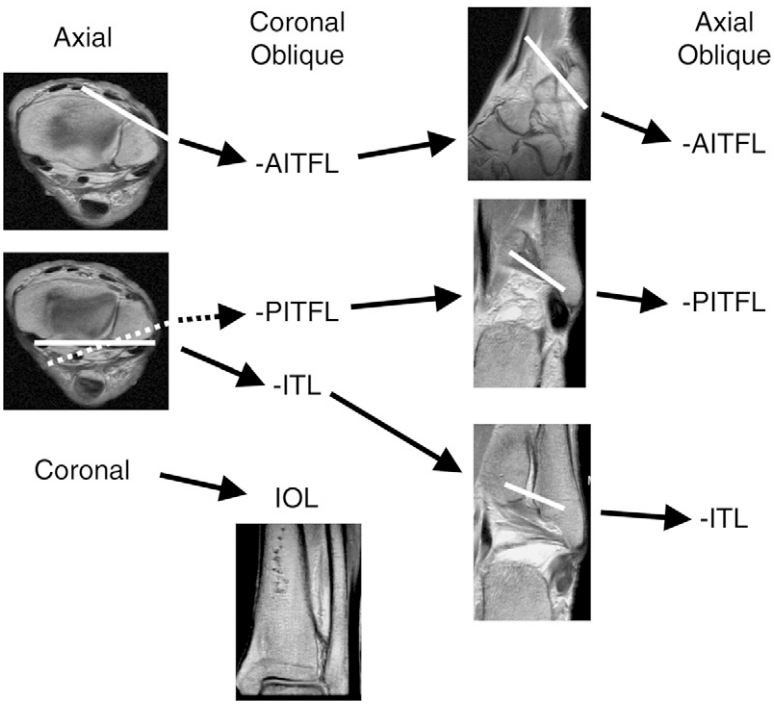


**Figure 1:** Flowchart shows the MR imaging protocol, which was performed with the ankle in the neutral position. Images were initially obtained in the axial and coronal planes. Images obtained in the coronal plane depicted the IOL. Images obtained in the axial plane were used to plan imaging in the coronal oblique plane, which was parallel to the AITFL, PITFL, and ITL. The axial oblique plane was programmed to be parallel to each ligament depicted in the coronal oblique plane. A total of nine sequences were performed. Each proton-density-weighted sequence required about 3 minutes to complete. The total imaging time was only 27 minutes.

AITFL and intermalleolar ligament (IML) were used for measurement, as they best demonstrated the entire length of the individual ligaments (Fig 2). The entire length of each ligament was measured from its proximal to its distal attachment. The width of the fascicles and gaps between fascicles were measured at their widest portions. The angle of each ligament was measured by using a line parallel to each ligament and another line parallel to the ankle joint line. The distance from the ankle joint line to the distal and proximal tibial attachments of the IOL was measured in the coronal plane.

### MR Anatomic Correlation

After completion of the MR examination, the cadaveric ankle specimens were again frozen at −40°C for a minimum of 120 hours. Three of the specimens were sliced in the oblique planes, corresponding to the MR imaging planes for each individual ligament. The remainders of the specimens were then sliced in the standard planes with a band saw (model B12; Butcher Boy, Reno, NV) into 3-mm-thick slices. After debris was rinsed from the surface of the specimens, the slices were thawed, and each slice was imaged with high-spatial-resolution radiography (Faxitron; Hewlett Packard, Palo Alto, Calif) and photographed under floodlights

**Figure 2**

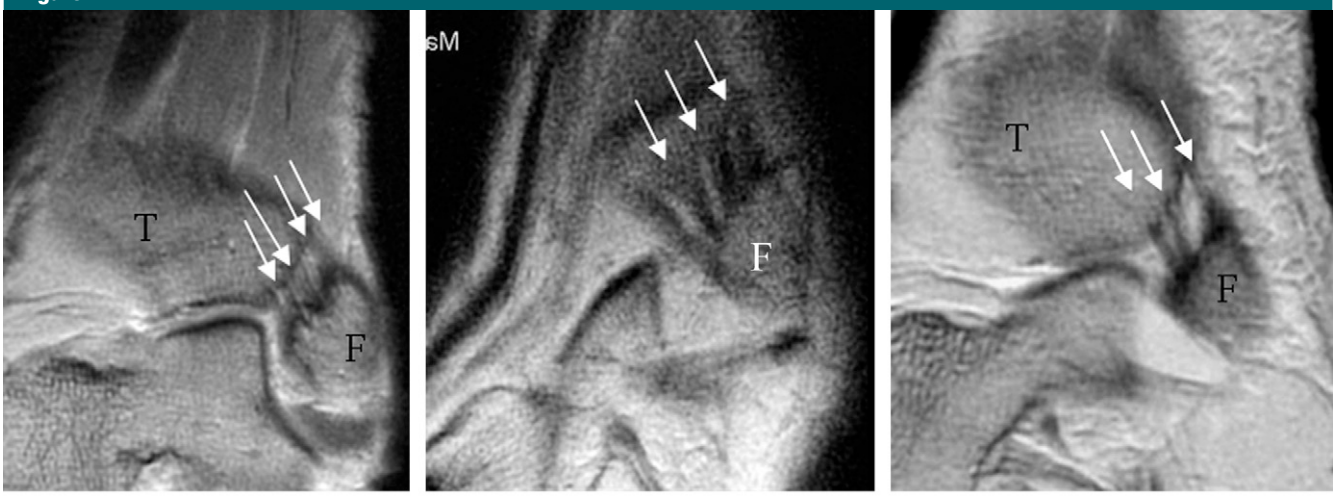


a. b. c.

**Figure 2:** **(a–c)** Coronal oblique proton-density-weighted MR arthrographic images (3000 images per minute) of AITFL obtained parallel to the long axis of the ligament. A variable number of bands of the AITFL (arrows) can be seen (four in **a**, three in **b** and **c**). *F* = fibula, *T* = tibia.

**Figure 3**

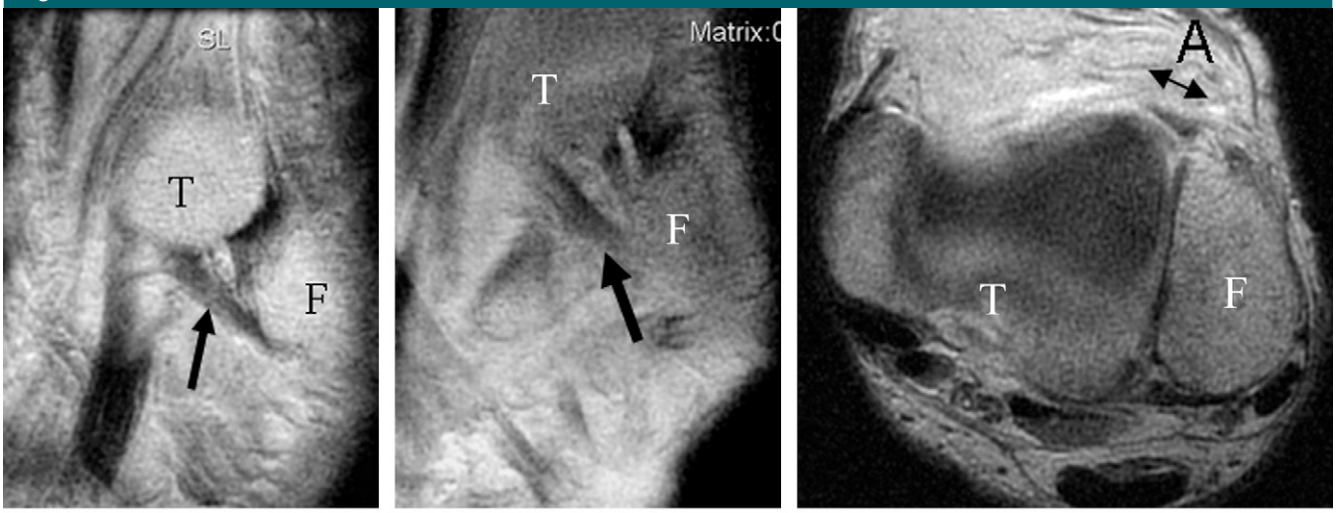


a. b. c.

**Figure 3:** **(a, b)** Coronal oblique proton-density-weighted MR arthrographic images (3000 images per minute) show the distal band of the AITFL (arrow). This band has a more horizontal orientation than does the main portion of the AITFL, thereby causing a triangular fat-filled gap. **(c)** Axial proton-density-weighted MR arthrographic image demonstrates distance A (*A*, double arrow), as described in Table 1. This distance was measured from the anteromedial tibial attachment of the distal fascicle to the medial distal tibia. *F* = fibula, *T* = tibia.

with a digital camera (Coolpix 990; Nikon, Tokyo, Japan). To determine the anatomic details of the syndesmotic ligaments, MR images of each specimen were correlated with findings derived during visual inspection of the anatomic slices.

## Results

### AITFL Findings

The AITFL had a trapezoidal shape, with multiple bands of fibers that extended obliquely in a distal and lateral direction from the tibia to the fibula. The course of the AITFL was best seen in the coronal oblique plane. This ligament had a variable number of bands, ranging from three to four. Each band was separated by fat. The middle part of the ligament was usually the widest and most anterior.

A separate distal band was seen in all specimens. This band had a triangular shape, which was wider at the tibial attachment and extended laterally in a distal direction to attach to the fibula. In several specimens, this distal band crossed the lateral corner of the talocrural joint. It had a tibial attachment that was more anterior and medial along the tibial plafond and a fibular attachment that was distal when compared with the other components of the AITFL. Measurements of distance A, the medial margin of the tibial attachment of this band to the lateral border of the distal tibia, ranged from 2.4 to 7.1 mm (mean, 5.3 mm ± 1.4 [standard deviation]) (Table 1). This band had a more horizontal course than did the remaining portions of the AITFL. The different orientation of the AITFL and the distal band resulted in a triangular gap filled with fat between these two structures (Fig 3). The widest part of this gap ranged from 1 to 3 mm (mean, 1.9 ± 0.04 mm) (Table 1).

**Table 1**

**Measurements of Distal Band of AITFL**

| Dimension | Maximum | Minimum | Mean ± Standard Deviation |
|---|---|---|---|
| Length (mm) | 23 | 7.8 | 14.5 ± 4.3 |
| Width (mm) | 4.3 | 1.7 | 3.0 ± 1.0 |
| Anteromedial tibial attachment* (mm) | 2.4 | 7.1 | 5.3 ± 1.4 |
| Gap from main AITFL (mm) | 3.0 | 1.0 | 1.9 ± 0.04 |
| Angle from joint line (degrees) | 65.2 | 39.5 | 52.2 ± 9.6 |
| Angle of AITFL (degrees) | 78 | 55.7 | 65.4 ± 7.2 |

* This was referred to as measurement A.

### PITFL Findings

The PITFL was a compact ligament that was triangular in shape and extended from the posterior edge of the fibular notch of the distal tibia to the malleolar fossa behind the triangular articular facet of the lateral malleolus of the fibula (Fig 4). The ligament was multifascicular, with a broad attachment to the lateral malleolus (Fig 5). It was more proximal and superficial to the ITL and extended in a more oblique direction (Fig 6). The superior margin of the PITFL was in close proximity to the IOL.

**Figure 4**

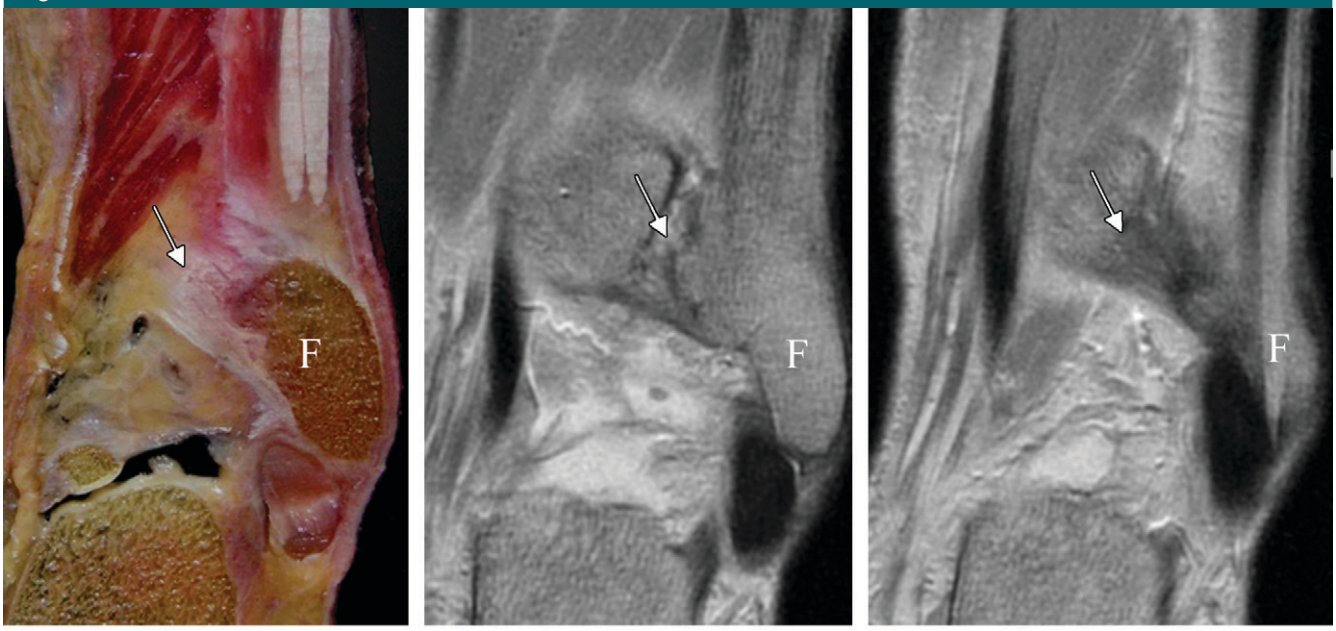


a. b. c.

**Figure 4:** **(a)** Coronal oblique section of cadaveric specimen shows vertical orientation and superficial location of the PITFL (arrow). **(b, c)** Corresponding coronal oblique proton-density-weighted MR arthrographic images (3000 images per minute) show the triangular shape of the PITFL (arrow). *F* = fibula.

**Figure 5**

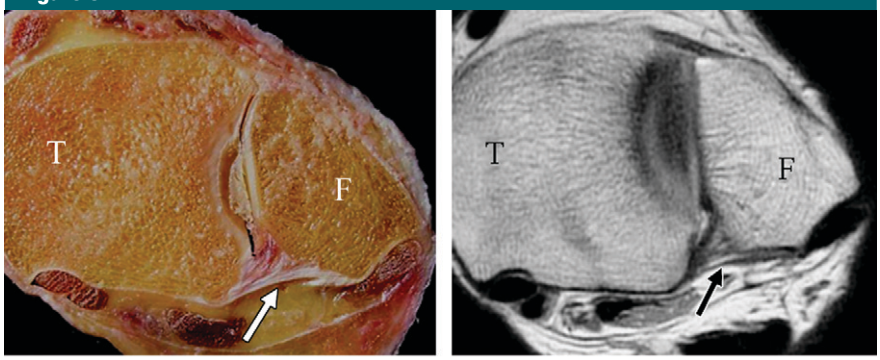


a. b.

**Figure 5:** **(a)** Axial oblique section of cadaveric specimen and **(b)** corresponding axial oblique proton-density-weighted MR arthrographic image (3000 images per minute) demonstrate triangular shape of PITFL. This ligament is multifascicular, with a broad attachment to the posterior edge of the lateral malleolus (arrow), which is behind the triangular articular facet. *F* = fibula, *T* = tibia.

### ITL Findings

The ITL, or the deep component of the PITFL, was a labrumlike extension of the posterior border of the tibial articular surface (Fig 7). The course of this ligament was more horizontal than that of the PITFL. This ligament originated above the malleolar fossa of the lateral malleolus just below the attachment of the PITFL (Fig 8). The ITL inserted on the posteroinferior corner of the fibular notch of the distal tibia.

### IML Findings

The IML was seen as a distinct separate ligament traversing between the posterior talofibular ligament (PTFL) and the ITL. On MR images, there was evidence of fat separating these three ligaments (Fig 9). The configuration of the IML was variable and ranged from a thin fibrous band to a thick cordlike structure. Some IMLs were fenestrated, resulting in a few separate fibers at their medial attachment, and some appeared as a single group of thin fibers (Fig 10). The IML was identified in all specimens. The length of this ligament is summarized in Table 2. On MR axial oblique images, the fibular attachment of the IML was well visualized and located above the PTFL. The IML originated laterally at a lower segment of the lateral malleolar fossa, near the superior border of the attachment of the PTFL. The insertion of the IML included the medial border of the medial malleolus through the septum between the flexor digitorum longus and the tibialis posterior tendons and the lateral border of the medial malleolar sulcus (Figs 9, 10). The course of the IML was oblique with respect to the posteromedial aspect of the ankle joint (Fig 9b).

### IOL Findings

The IOL was located between the fibular notch of the tibia and the medial aspect of the distal fibula. It was a broad

**Figure 6**

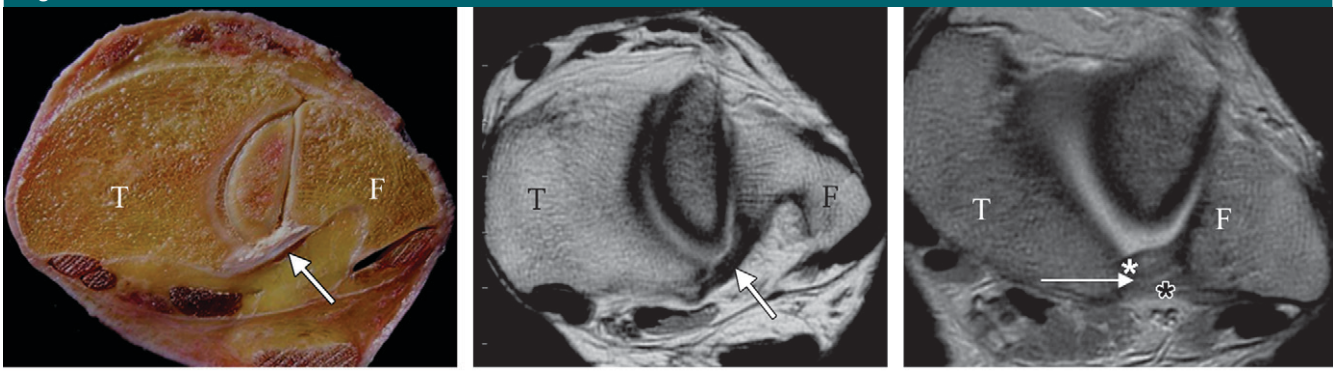


a. b. c.

**Figure 6:** **(a)** Axial oblique slice of a cadaveric specimen and **(b)** corresponding axial oblique proton-density-weighted MR arthrographic image (3000 images per minute) show that the ITL (arrow) originates above the digital fossa of the lateral malleolus just below the PITFL. The ITL inserts on the posteroinferior corner of the fibular notch of the distal tibia. **(c)** Axial oblique proton-density-weighted MR image shows fat signal intensity (arrow), which separates the PITFL (white asterisk) and ITL (black asterisk). *F* = fibula, *T* = tibia.

and multifascicular ligament, traveling obliquely from its proximal tibial attachment to its distal fibular attachment. The anterior fibers were more proximal, and the posterior fibers were more distal. The posterior fibers were located in close proximity to the superior margin of the PITFL (Fig 11). The distance between the joint line and the proximal tibial attachment of the IOL ranged from 31.4 to 44.0 mm (mean, 37.7 mm ± 4.6) (Table 3). The most proximal fibers of the IOL attached to the tibia at the top of the fibular notch. The distance between the distal attachment of this ligament and the joint line ranged from 16.2 to 33.1 mm (mean, 24.0 mm ± 4.8). Coronal and axial MR imaging planes best depicted the orientation of this ligament.

**Figure 7**

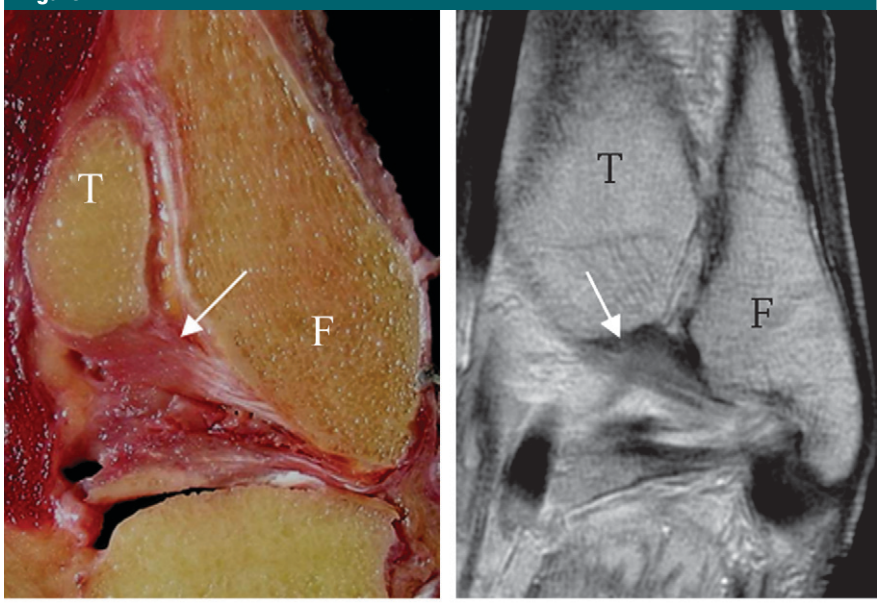


a. b.

**Figure 7:** **(a)** Coronal oblique section of cadaveric specimen and **(b)** coronal oblique proton-density-weighted MR arthrographic image (3000 images per minute) show the labrumlike appearance of the ITL. The normal ITL (arrow) courses in a horizontal oblique direction and inserts on the posteroinferior segment of the fibular notch. *F* = fibula, *T* = tibia.

## Discussion

The tibiofibular syndesmotic ligaments are important to the stability of the ankle joint. To assess the detailed anatomy of these ligaments, we performed MR imaging in standard and oblique planes parallel to the long axis of these ligaments. In our study, these ligaments were depicted in full length from their proximal to distal attachments by using these oblique planes. Lee et al (6) studied ankle ligaments with MR arthrography in the axial, axial oblique, coronal, and sagittal planes, but they were unable to visualize the entire length of the AITFL. Muhle et al (5) used coronal planes with the foot in 40°–50° of plantar flexion to enable visualization of the multifascicular appearance of the AITFL in three of six specimens. In our study, we performed MR imaging in the coronal oblique plane with the ankle in the neutral position to visualize the entire extent of the AITFL in all 10 specimens. The middle part was the widest component of this ligament, a finding that was in agreement with the findings of the anatomic study of Ebraheim et al (7). The middle band of the AITFL was also the most anterior part, originating from the anterior tubercle of the distal tibia and attaching to the

**Figure 8**

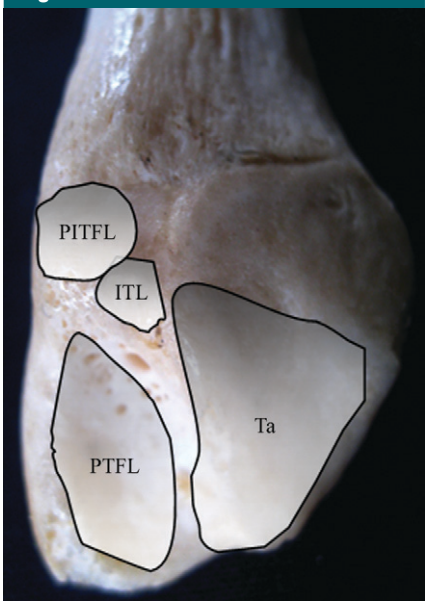


**Figure 8:** The osseous anatomy shows the inner surface of the malleolar fossa of the lateral malleolus, which is congruent with the fibular groove of the distal tibia and the talus *(Ta)*. Areas of gray shadow show the relationship between the PITFL, ITL, and PTFL in the malleolar fossa. The PTFL occupies the distal segment of the concavity of this groove, whereas the fiber of the ITL is located above and slightly anterior to the PTFL and filled-in proximal segment of the groove. The PITFL is inserted superoposterior to the ITL.

**Figure 9**

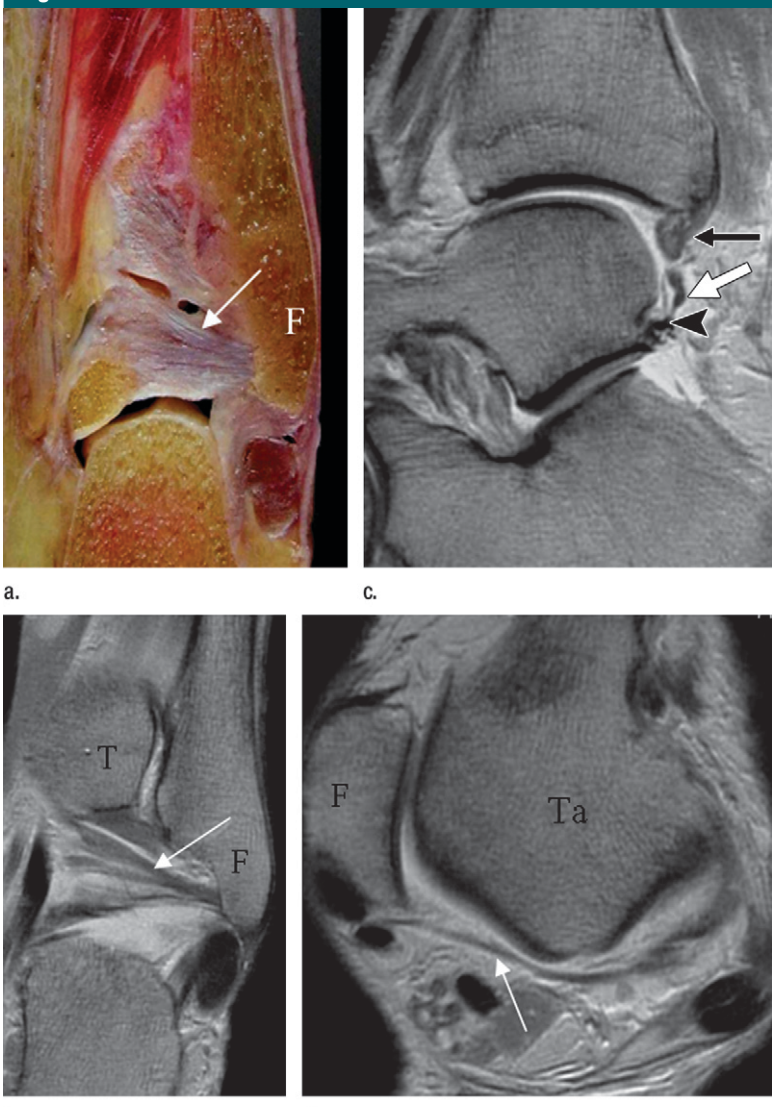


**Figure 9:** **(a)** Coronal oblique slice of cadaveric specimen and **(b)** corresponding coronal oblique MR arthrographic image (3000 images per minute) show cordlike appearance of the IML. **(c)** Sagittal MR arthrographic image (3000 images per minute) shows the location of the IML (white arrow) between the ITL (black arrow) and PTFL (black arrowhead). **(d)** Axial oblique MR arthrographic image (3000 images per minute) shows that the course of the IML is horizontal and oblique, with respect to the posteromedial aspect of the ankle joint, at the level of talus. *F* = fibula, *T* = tibia, *Ta* = talus.

superior part of the anterior tubercle of the fibula (7). In addition to stabilizing the distal tibiofibular articulation, the AITFL prevents excessive movement of the fibula and external rotation of the talus (8,9).

In several of our specimens, the distal band of the AITFL crossed the talocrural joint. Serrafian (2) indicated that the lowest fibers of the AITFL are in close proximity to the origin of the anterior talofibular ligament. We visualized this distal band in all specimens by using the coronal oblique imaging plane. Akseki et al (10) termed this band the distal fascicle and found that it was present in 39 (82.9%) of 47 specimens. This is in accordance with the results of our study and those reported by Bassett et al (90.9%) (11). Ray and Kriz (12), however, found this ligament to be present in only 10 of 46 specimens. This discrepancy may be related to the fact that Ray and Kriz excluded the presence of a separate fascicle if any digitations were found between the fascicle and the main body of the AITFL. In our study, this band had a more horizontal course than did the AITFL. Akseki et al (10) concluded that if the fibular attachment of this band was more distal to the joint line, the fascicle had the potential to cause symptomatic impingement at the anterolateral aspect of the talar dome. We found that in specimens in which this band had a more anterior and medial attachment to the tibia plafond or a greater value of distance A, the band crossed the talocrural joint and, at the very least, had the potential to cause disease.

**Figure 10**


a. b. c. d.

**Figure 10:** Coronal oblique proton-density-weighted MR arthrographic images (3000 images per minute) of several specimens show variable configurations of the IML. *F* = fibula, *T* = tibia. **(a)** The multifascicular band with trifurcation of the fibers at the medial attachment of the IML (arrow) can be seen. **(b, c)** The thick cord (**b**) and thin fiber (**c**) of the IML (arrow) can be seen. **(d)** The thin fiber of the IML at the fibular attachment can be seen. This fiber courses horizontally oblique and becomes a thick band at the medial attachment (arrow).

**Table 2**

**Length of IML from Coronal Oblique Plane Parallel to ITL**

| Value | Length (mm) |
|---|---|
| Maximum | 39.7 |
| Minimum | 22.0 |
| Mean ± standard deviation | 31.5 ± 6.0 |

Muhle et al (5) studied the PITFL with the foot in both dorsiflexion and plantar flexion. In four of their six specimens, these investigators were unable to distinguish the PITFL from the ITL. In our study, we used coronal and axial oblique imaging planes parallel to each ligament with the foot in neutral position. These two ligaments could be differentiated by the fat signal between the ligament fibers.

The IML, while clinically important, has been largely neglected in most anatomy textbooks (2,13). There is a brief mention of the ligament in the anatomic and orthopedic literature, in which it has been touted as a cause of posterior impingement syndrome (14). The results of current studies have shown that this ligament is a distinct structure, located between the PTFL and ITL. In the reports of anatomic studies, the IML was seen in 56% (20 of 36 specimens), 72% (29 of 40 specimens), and 82% (63 of 77 specimens) of specimens, respectively (14–16). Rosenberg et al (14) found the IML in 18 (19%) of 97 MR examinations and used its characteristic fibular and tibial attachments to aid in indentifying this ligament in standard imaging planes. Oh et al (16) were able to identify the IML in all MR imaging studies (26 specimens) with standard imaging planes. In our study, the IML was seen in all specimens in the coronal oblique plane. In addition, the standard sagittal plane also enabled identification of the IML as a thick fibrous cord between the ITL and the PTFL. The configuration of the IML is variable, ranging from a thin set of fibers to a thick compact band. Rosenberg et al (14) found that the ligament split into two or three different bands in seven (20%) of 36 specimens. In two anatomic studies, researchers found that the average length of the IML was 23.5 mm (15) and 23 mm (17), while in our study, we found the average length of the IML was 32 mm. This discrepancy in the length of the IML was perhaps related to visualization of the entire ligament in the oblique plane in our study. Rosenberg et al (14) found the IML to be bilateral in five (16%) of 32 MR examinations. In our study, we found the incidence of bilateral IML to be 25% (two of eight cadavers), although this population was too small to enable us to draw conclusions from this discrepancy.

The IOL originates from the anteroinferior triangular segment of the medial aspect of the distal fibular shaft (1). Monk (17) found a variable attachment of the IOL that ranged from 2–6 cm above the ankle. Our results showed that the most distal fibers of the IOL are located more posteriorly within the distal tibiofibular space and attached to the tibia 2–3 cm proximal to the level of the joint line, whereas

**Figure 11**

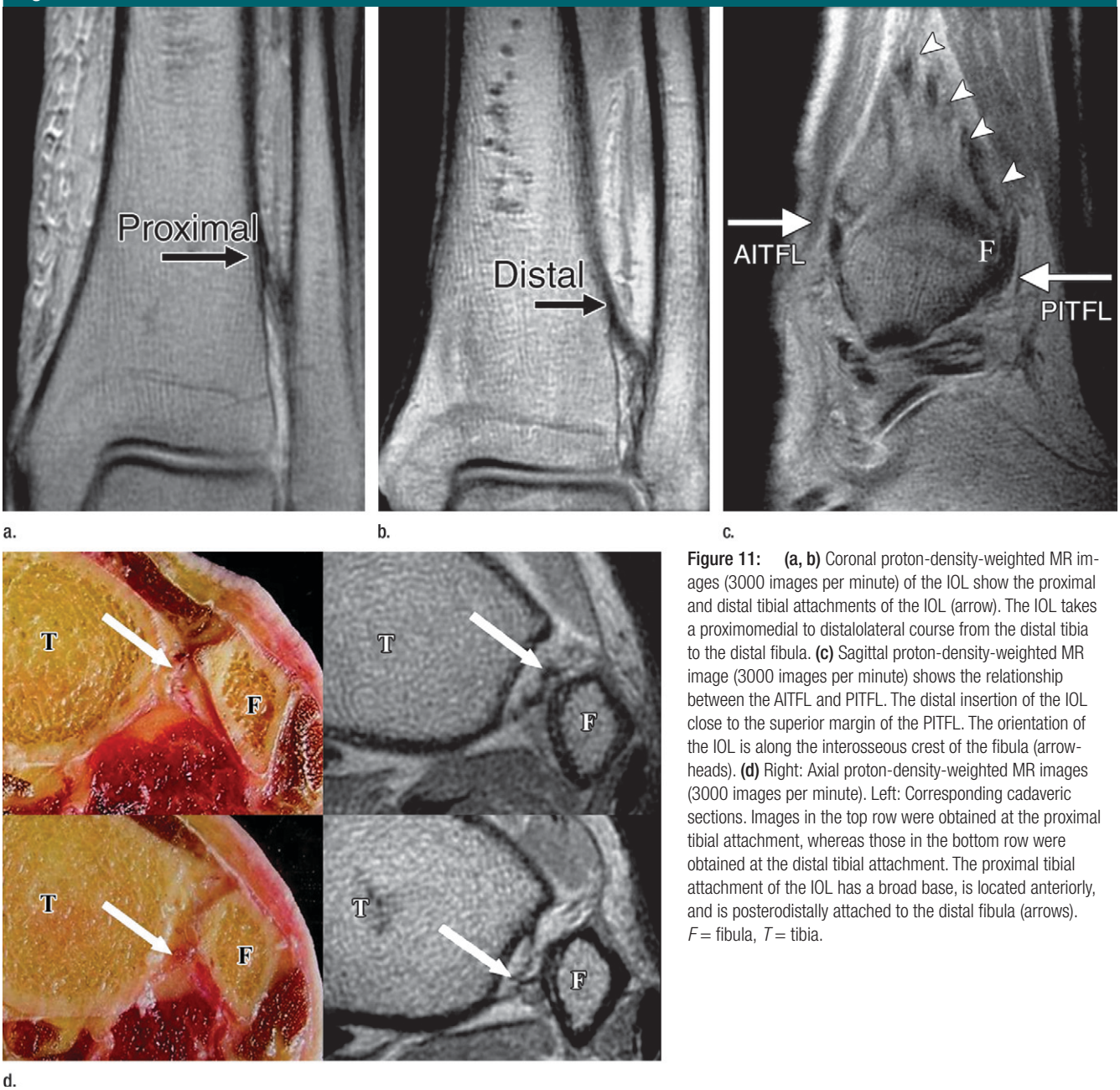


**Figure 11:** **(a, b)** Coronal proton-density-weighted MR images (3000 images per minute) of the IOL show the proximal and distal tibial attachments of the IOL (arrow). The IOL takes a proximomedial to distalolateral course from the distal tibia to the distal fibula. **(c)** Sagittal proton-density-weighted MR image (3000 images per minute) shows the relationship between the AITFL and PITFL. The distal insertion of the IOL close to the superior margin of the PITFL. The orientation of the IOL is along the interosseous crest of the fibula (arrowheads). **(d)** Right: Axial proton-density-weighted MR images (3000 images per minute). Left: Corresponding cadaveric sections. Images in the top row were obtained at the proximal tibial attachment, whereas those in the bottom row were obtained at the distal tibial attachment. The proximal tibial attachment of the IOL has a broad base, is located anteriorly, and is posterodistally attached to the distal fibula (arrows). *F* = fibula, *T* = tibia.

the anterior fibers had a broad attachment to the tibia more proximally. The ligament coursed obliquely to attach to the fibula just above the talocrural joint. We also found that the distal part of this ligament bordered the superior edge of the PITFL. The most proximal fibers attached to the tibia at the level of the top of the fibular notch.

**Table 3**

**Distance from Joint Line to Tibial Attachments of IOL**

| Attachment | Maximum (mm) | Minimum (mm) | Mean ± Standard Deviation (mm) |
|---|---|---|---|
| Proximal tibial | 44.0 | 31.4 | 37.7 ± 4.6 |
| Distal tibial | 33.1 | 16.2 | 24.0 ± 4.8 |

We observed that the IOL ran obliquely in a proximomedial to distalolateral direction from the distal tibia to the distal fibula. This oblique orientation may facilitate translational and rotational motion of the distal tibiofibular articulation (18).

Our study had several limitations. The number of specimens was small without significant clinical data, limiting the significance and clinical correlation of our conclusions. The advanced age of the donors at time of death also may have resulted in the inclusion of many specimens with degenerative changes. The measurements were obtained by only one observer; however, they were obtained three times, and an average value was calculated. We used nonstandard oblique planes that are not typically used in clinical practice. Our results, however, suggest that such oblique planes improve visualization of the syndesmotic ligaments and, at least potentially, could be beneficial when MR imaging is used to evaluate the injured ankle. With improvements in three-dimensional volume-acquired imaging techniques, reconstruction rather than direct imaging in oblique orientations may be of value in the future.

In conclusion, oblique MR imaging planes angulated parallel to the long axis of each ligament can optimize visualization of the normal tibiofibular syndesmotic ligaments. However, future studies are required to further evaluate any potential clinical application of MR imaging with oblique planes in the assessment of the syndesmotic ligaments.

## References

1. Takao M, Ochi M, Oae K, Naito K, Uchio Y. Diagnosis of a tear of the tibiofibular syndesmosis: the role of arthroscopy of the ankle. J Bone Joint Surg Br 2003;85:324–329.
2. Serrafian SK. Syndesmology. In: Sarrafian SK, ed. Anatomy of the foot and ankle. 2nd ed. Philadelphia, Pa: Lippincott, 1993; 159–217.
3. Resnick DL, Kang HS, Pretterklieber ML, eds. Ankle and foot. In: Internal derangements of joints. 2nd ed. Philadelphia, Pa: Saunders, 2007; 2012–2116.
4. Vogl TJ, Hochmuth K, Diebold T, et al. Magnetic resonance imaging in the diagnosis of acute injured distal tibiofibular syndesmosis. Invest Radiol 1997;32:401–409.
5. Muhle C, Frank LR, Rand T, et al. Tibiofibular syndesmosis: high resolution MRI using a local gradient coil. J Comput Assist Tomogr 1998;22:938–944.
6. Lee SH, Jacobson J, Trudell D, Resnick D. Ligament of ankle: normal anatomy with MR arthrography. J Comput Assist Tomogr 1998;22:807–813.
7. Ebraheim NA, Taser F, Shafiq Q, Yeasting RA. Anatomical evaluation and clinical importance of the tibiofibular syndesmosis ligaments. Surg Radiol Anat 2006;28: 142–149.
8. Dattani R, Patnaik S, Kantak A, Srikanth B, Selvan TP. Injuries to the tibiofibular syndesmosis. J Bone Joint Surg Br 2008;90: 405–410.
9. Sarsam IM, Hughes SP. The role of the anterior tibiofibular ligament in talar rotation: an anatomical study. Injury 1988;19:62–64.
10. Akseki D, Pinar H, Yaldiz K, Akseki NG, Arman C. The anterior inferior tibiofibular ligament and talar impingement: a cadaveric study. Knee Surg Sports Traumatol Arthrosc 2002;10:321–326.
11. Bassett FH 3rd, Gates HS 3rd, Billys JB, Morris HB, Nikolaou PK. Talar impingement by the anterior inferior tibiofibular ligament. J Bone Joint Surg Am 1990;72:55–59.
12. Ray RG, Kriz BM. Anterior inferior tibiofibular ligament: variations and relationship to the talus. J Am Podiatr Med Assoc 1991;81:479–485.
13. Williams PL, Warwick R, Dyson M, Bannister LH, eds. Gray's anatomy. 37th ed. New York, NY: Churchill Livingstone, 1989; 161:831–836.
14. Rosenberg ZS, Cheung YY, Beltran J, Sheskier S, Leong M, Jahss M. Posterior intermalleolar ligament of ankle: normal anatomy and MR imaging features. AJR Am J Roentgenol 1995;165:387–390.
15. Milner CE, Soames RW. Anatomy of the collateral ligaments of the human ankle joint. Foot Ankle Int 1998;19:757–760.
16. Oh CS, Won HS, Hur MS, et al. Anatomic variations and MRI of the intermalleolar ligament. AJR Am J Roentgenol 2006;186:943–947.
17. Monk CJ. Injuries of the tibio-fibular ligaments. J Bone Joint Surg Br 1969;51:330–337.
18. Skraba JS, Greenwald AS. The role of the interosseous membrane on tibiofibular weightbearing. Foot Ankle 1984;4:301-304.